Preprints of the 21st IFAC World Congress (Virtual)
Berlin, Germany, July 12-17, 2020

Active Vibration Control of a Convertible Structure based on a Polytopic LPV Model Representation

Robert Jirasek * **Thomas Schauer** ** **Achim Bleicher** *

* *Chair of Hybrid Structures - Structural Concrete, Brandenburg University of Technology, 03046 Cottbus, Germany, (e-mail: jirasek@b-tu.de)*
** *Control Systems Group, Technische Universität Berlin, 10587 Berlin, Germany*

Abstract: This paper deals with modeling and control of lightweight convertible structures for the application in civil and structural engineering. Such structures are prone to vibrations due to their lightweight design. In addition, they exhibit transformation state dependent dynamic behavior. In order to guarantee a reliable operation, the use of active vibration control (AVC) is an effective means. For the example of a simplified convertible structure, modeling is demonstrated using the linear parameter-varying (LPV) framework. Based on local linear time-invariant (LTI) models, derived from a finite element model of the convertible structure, a polytopic LPV model is established. This LPV model is then utilized to design a polytopic LPV output-feedback controller for AVC during the structure's transformation. The effectiveness of the designed controller is validated in simulation.

Keywords: Convertible structures, Active vibration control, Linear parameter-varying systems

1. INTRODUCTION

Convertible structures in civil and structural engineering are mainly designed for roofs, bridges and facade systems. With respect to the energy needed to transform such structures, a lightweight design is highly desirable. *Elastic kinetic structures*, which are based on the approach of active-bending, are of growing interest in the field of lightweight convertible structures (Lienhard et al. (2013)). Concepts for applications range from adaptive facade systems through pavilions to convertible stadium roofs (Vergauwen et al. (2017), Körner et al. (2018), Takahashi et al. (2016)). In the first place, current investigations focus on the principles of transformation. However, due to their lightweight design, these structures are highly sensitive to static and dynamic loads, e.g. induced by wind. Consequently, an adaption for static and dynamic loads seems to be reasonable for a reliable operation under real-world conditions. For lightweight but *non-convertible* structures the static and dynamic load adaptation has been investigated by, e.g. Senatore et al. (2018), Neuhäuser et al. (2013) and Bleicher et al. (2011), and was proven to be very effective.

In our current research we are focusing on the development and realization of lightweight convertible structures based on active-bending with controlled transformation and simultaneous vibration mitigation for real-world applications (e.g. multi-functional pavilions, convertible roofs). The considered structures exhibit geometrical nonlinearities, due to large transformations. Modeling in the classical linear time-invariant (LTI) framework is thus not expedient. For this reason, in (Jirasek et al. (2019b)), modeling of a simplified actuated convertible structure was carried out in the linear parameter-varying (LPV) framework. The derived grid-based LPV model was validated in simulation by comparison with data from a non-linear transient analysis of a finite element model, which proved the feasibility of the LPV framework for modeling. In (Jirasek et al. (2019a)) the existing model was extended by means of an active vibration control (AVC) of the first and second mode. Single-input single-output (SISO) control design was carried out with the root locus method using the same control input under the assumption of well separated eigenfrequencies. The implemented AVC was then validated in simulation. However, the SISO control design on the basis of the grid-based LPV model neither guarantees stability nor performance. In order to guarantee stability and performance inherently with the controller design, appropriate LPV approaches have to be utilized. An overview on LPV control approaches with applications is given by the survey of Hoffmann and Werner (2015), for an in-depth view with application examples we refer to the book of Mohammadpour and Scherer (2012).

This contribution improves our previous work with respect to methodological issues by (i) the derivation of an LPV model in polytopic form, which allows (ii) synthesis of an polytopic LPV output-feedback controller with guarantees on stability and $\mathcal{H}_\infty$ performance γ between disturbance input and performance output.

This paper is organized as follows: Section 2 briefly describes the considered convertible structure. In Section 3 the derivation of an LPV model in polytopic form is explained in detail. Section 4 describes the LPV control

design and in Section 5 simulation results are depicted. The paper ends with a discussion of the results and an outlook for future work in Section 6.

2. SYSTEM DESCRIPTION

2.1 Lightweight Convertible Structure

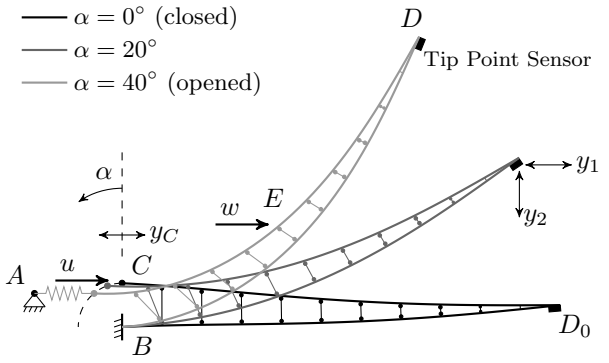

Fig. 1. Structure in different transformation states under self-weight (note that for reasons of simplicity the spring is visible in the opened state only).

The lightweight convertible structure considered throughout this paper is illustrated in Fig. 1. The special property of this structure is, that small movements of the actuated support C generate large transformations of the tip point D. The two cantilevered beams are connected by ten equally distributed pin-jointed links. The supports A and B are fixed in position, whereas support C can move on a circular path with a constant distance to B, which minimizes restraint forces at the supports. Support A and C are spring-connected. The spring constant is chosen such that the self-weighted structure is kept in its opened transformation state. Applying an actuation force u at C in horizontal direction, the structure can be transformed and brought into the closed transformation state. As a measure of transformation, we use the rotation angle

$$\alpha = \sin^{-1}(-y_C/\overline{BC}), \tag{1}$$

which is given by the relation between y_C, the horizontal movement of C, and the constant distance between B and C. In order to analyze the structure's dynamic behavior under disturbances a disturbance force w can be applied at point E. The structure's response is measured by two virtual sensors. The first sensor is attached at C, to measure the point's horizontal movement y_C and to allow the calculation of the transformation angle α. The second sensor provides the velocities y_1 and y_2 of the tip point D.

Table 1 contains the dimensional and material properties of the structure. As material for the structure carbon fiber reinforced plastic (CFRP) is used. The analysis and dimensioning was conducted on the basis of a finite element model, which was introduced in (Jirasek et al. (2019b)).

2.2 Modal Analysis

The results of a modal analysis, which was conducted in (Jirasek et al. (2019b)) are illustrated in Fig. 2 and are briefly summarized in the following. In the first mode shape the spring vibrates, which leads to a vibration of the whole structure. The remaining three mode shapes are classical vertical bending modes, which qualitatively do not change during the transformation. However, due to a change of geometrical stiffness and mass distribution, they show slight quantitative variations and, more significant, a change of the eigenfrequencies for these three mode shapes can be observed (see Tab. 2). This transformation state dependent dynamic behavior motivates the use of the LPV framework for modeling, which is described in the next section.

Table 1. Dimensional and material properties of the convertible structure.

Dimensional Properties	
Length $\overline{BD_0}$	7.5 m
Support Distance $\overline{BC}$	0.75 m
Structure Width d	0.2 m
Beam Cross Section Thickness b	10 mm
Link Cross Section Thickness l	5 mm

Material Properties	
Density CFRP ν	1.6 kg/dm^3
Flexural Young's Modulus CFRP E	165000 N/mm^2
Flexural Strength CFRP σ	2800 N/mm^2
Spring Constant k	10.31 N/mm

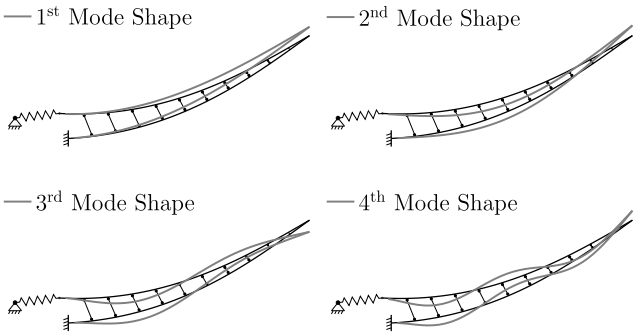

Fig. 2. Plot of the first four mode shapes for a transformation state of $\alpha = 20°$ (links are neglected for the mode shapes).

Table 2. Change of eigenfrequencies over transformation (↑ indicates increasing and ↓ decreasing frequency) and absolute frequency change (Δf).

Transformation [°]	Frequency [Hz]			
α	f_1	$f_2 \downarrow$	$f_3 \uparrow \& \downarrow$	$f_4 \downarrow$
0	0.52	1.76	4.80	9.36
10	0.52	1.71	4.83	9.27
20	0.52	1.66	4.81	9.16
30	0.52	1.61	4.74	9.03
40	0.52	1.57	4.64	8.91
$\lvert\Delta f\rvert$	-	0.19	0.19	0.45

3. LPV MODELING

3.1 Overview

Before a formal introduction of LPV systems and the detailed derivation of the LPV model for the convertible structure, an overview of the interaction between LPV

model and LPV controller is given in Fig. 3. The LPV

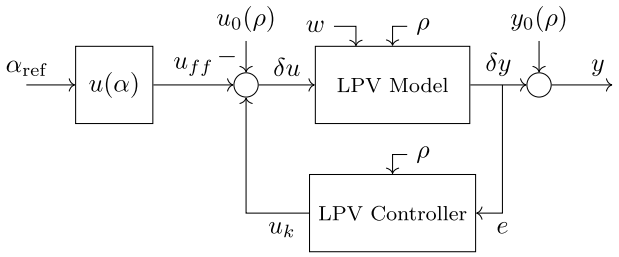

Fig. 3. Structure of LPV model and LPV controller with inputs and outputs.

model, the LPV controller and the local equilibrium input force $u_0(\rho)$ and output values $y_0(\rho)$ depend on the current transformation state of the structure, which is represented by the scheduling parameter ρ (introduced later). At this point, it is emphasized that the LPV model describes *deviations* from the current transformation state of the structure. Hence, the model is based on a local input δu and provides local outputs δy. The local input is made up of a feed-forward force u_{ff}, which realizes a certain transformation trajectory α_{ref}, a control force u_k and the local equilibrium force $u_0(\rho)$, which is subtracted. The global outputs y are given as the sum of local outputs δy and local equilibrium output values $y_0(\rho)$. Moreover, the LPV model is subject to the disturbance force w. The LPV controller generates a control force u_k on the basis of the velocities at the tip point (y_1 and y_2), which are stored in δy. Please note that the velocity values are also global, as their local equilibrium values are always zero and thus $y = \delta y$ in case of velocity measurements only. By this velocity feedback, the controller introduces additional "active" damping into the structure.

In the following, LPV systems are introduced and the LPV model of the structure is derived in polytopic form.

3.2 Polytopic LPV Systems

For an introduction to the different representations of LPV systems refer to, e.g. Briat (2015). A general LPV system in state-space description with notation referring to Fig. 3 (and neglecting the input disturbance w) can be given by

$$\begin{bmatrix} \dot{x}(t) \\ \delta y(t) \end{bmatrix} = \begin{bmatrix} A(\rho(t)) & B(\rho(t)) \\ C(\rho(t)) & D(\rho(t)) \end{bmatrix} \begin{bmatrix} x(t) \\ \delta u(t) \end{bmatrix} \tag{2}$$

with $\rho = [\rho_1 \ \rho_2 \dots \rho_{n_\rho}]^T \in \mathcal{P} \subseteq \mathbb{R}^{n_\rho}$ the vector of time-varying scheduling parameters, $x \in \mathbb{R}^{n_x}$ the state vector, $\delta u \in \mathbb{R}^{n_u}$ the vector of inputs, $\delta y \in \mathbb{R}^{n_y}$ the vector of outputs, and the continuous matrix valued functions of the scheduling parameter vector $A : \mathbb{R}^{n_\rho} \to \mathbb{R}^{n_x \times n_x}$, $B : \mathbb{R}^{n_\rho} \to \mathbb{R}^{n_x \times n_u}$, $C : \mathbb{R}^{n_\rho} \to \mathbb{R}^{n_y \times n_x}$, and $D : \mathbb{R}^{n_\rho} \to \mathbb{R}^{n_y \times n_u}$. In general it is assumed that the scheduling trajectories take on values in a known compact set $\mathcal{P}$ and that they are rate bounded, meaning $\dot{\rho}_{min} \leq \dot{\rho} \leq \dot{\rho}_{max}$ with $\dot{\rho}_{min}$ and $\dot{\rho}_{max} \in \mathbb{R}^{n_\rho}$.

An LPV system is called polytopic, when (i) the parameter vector ρ varies in a fixed polytope $\mathcal{P}$ and (ii) the parameter dependence of the state-space matrices is affine. If the parameter vector ranges in a polytope $\mathcal{P}$ with M vertices $\rho_{vi} \in \mathbb{R}^{n_\rho}$ and $i = 1, 2, \dots, M$, an arbitrary point $\rho_a \in \mathcal{P}$ can be written as the convex combination of the vertices

$$\rho_a = \sum_{i=1}^{M} \lambda_i \rho_{vi}, \quad \lambda_i \geq 0, \ \sum_{i=1}^{M} \lambda_i = 1, \tag{3}$$

with the convex coordinates λ_i. In the case of affine dependence of the state-space matrices on the parameter vector, e.g. for the system matrix A

$$A(\rho) = \mathcal{A}_0 + \rho_1 \mathcal{A}_1 + \rho_2 \mathcal{A}_2 + \dots + \rho_{n_\rho} \mathcal{A}_{n_\rho}, \tag{4}$$

the state-space matrices range over a polytope of matrices with the vertices, e.g. $A_{vi} = A(\rho_{vi})$ for the system matrix. Thus, the system matrix can be represented as

$$A(\rho) = \lambda_1 A_{v1} + \lambda_2 A_{v2} + \dots + \lambda_M A_{vM} = \sum_{i=1}^{M} \lambda_i A_{vi}. \tag{5}$$

Consequently, the state-space matrices of a polytopic LPV system can be calculated from the M vertices of the polytope $\mathcal{P}$ by solving for the convex coordinates λ_i in (3) for a given ρ_a. The state-space matrices in polytopic LPV form can be written as

$$\begin{bmatrix} A(\rho) & B(\rho) \\ C(\rho) & D(\rho) \end{bmatrix} = \sum_{i=1}^{M} \lambda_i \begin{bmatrix} A_{vi} & B_{vi} \\ C_{vi} & D_{vi} \end{bmatrix}. \tag{6}$$

In the following, the steps required to derive a polytopic LPV model of the convertible structure are described.

3.3 Local LTI Models

In a first step, local LTI models are derived for discrete transformation states α using the finite element model of the convertible structure. The local models are of the form

$$M(\alpha)\delta\ddot{x}_n(t) + K(\alpha)\delta x_n(t) = B_u \delta u(t) + B_w w(t) \tag{7}$$

with $\delta x_n(t) \in \mathbb{R}^n, \delta x_n(t) = x_n(t) - x_0(\alpha)$ the vector of local deflections in nodal coordinates, $\delta\ddot{x}_n \in \mathbb{R}^n, \delta\ddot{x}_n(t) = \ddot{x}_n(t) - \ddot{x}_0(\alpha)$ the vector of local accelerations in nodal coordinates, $M(\alpha) \in \mathbb{R}^{n \times n}$ and $K(\alpha) \in \mathbb{R}^{n \times n}$ the mass and stiffness matrix at α, $B_u \in \mathbb{R}^n$ and $B_w \in \mathbb{R}^n$ the input matrices distributing actuation and disturbance inputs to the corresponding nodes and $\delta u \in \mathbb{R}^u, \delta u(t) = u(t) - u_0(\alpha)$ the local actuation input and $w(t) \in \mathbb{R}^w$ the disturbance input. This model describes deviations from the local equilibrium point α, which is given by the input force $u_0(\alpha)$, the deflection $x_0(\alpha)$ and the acceleration $\ddot{x}_0(\alpha) = 0$. System (7) is of high order ($n = 619$) and is thus reduced by means of modal reduction by the projection $\delta x_n = \Phi(\alpha)\delta x_m$, with the modal matrix $\Phi(\alpha) = [\phi_{\alpha,1} \ \phi_{\alpha,2} \dots \phi_{\alpha,n_{red}}] \in \mathbb{R}^{n \times n_{red}}$ consisting of the mode shapes $\phi_{\alpha,i} \in \mathbb{R}^n$ to be retained and the modal states $\delta x_m \in \mathbb{R}^{n_{red}}$. This results in the reduced system

$$\underbrace{\Phi^T M \Phi}_{I}\delta\ddot{x}_m(t) + \underbrace{\Phi^T K \Phi}_{\Omega^2(\alpha)}\delta x_m(t) = \Phi^T B_u \delta u(t) + \Phi^T B_w w(t), \tag{8}$$

where $\Omega^2(\alpha) = \text{diag}\{\omega_i^2(\alpha)\}$ is the diagonal matrix of squared angular frequencies. Rewriting (8) into modal state-space form and implementing modal damping $Z(\alpha) = \text{diag}\{2\zeta_i(\alpha)\omega_i(\alpha)\}$, with the modal damping ratio $\zeta_i(\alpha)$ corresponding to the i-th mode shape at α, yields

$$\underbrace{\begin{bmatrix} \delta\dot{x}_m \\ \delta\ddot{x}_m \end{bmatrix}}_{\dot{x}} = \underbrace{\begin{bmatrix} 0 & I \\ -\Omega^2 & -Z \end{bmatrix}}_{A(\alpha)} \underbrace{\begin{bmatrix} \delta x_m \\ \delta\dot{x}_m \end{bmatrix}}_{x} + \underbrace{\begin{bmatrix} 0 \\ \Phi^T B_u \end{bmatrix}}_{B_1(\alpha)} \delta u + \underbrace{\begin{bmatrix} 0 \\ \Phi^T B_w \end{bmatrix}}_{B_2(\alpha)} w. \tag{9}$$

The output equation to measure the support position y_C and the velocities y_1 and y_2 (refer to Fig. 1) is given by

$$\underbrace{\begin{bmatrix} y_C \\ \hline y_1 \\ y_2 \end{bmatrix}}_{y} = \underbrace{\underbrace{\left[\begin{array}{cc} C_s^p\Phi & 0 \\ \hline 0 & C_s^v\Phi \end{array}\right]}_{C(\alpha)} \begin{bmatrix} \delta x_m \\ \delta \dot{x}_m \end{bmatrix}}_{\delta y} + \underbrace{\begin{bmatrix} y_0^C(\alpha) \\ \hline 0 \\ 0 \end{bmatrix}}_{y_0(\alpha)}, \tag{10}$$

with $y \in \mathbb{R}^{n_y^p+n_y^v}$ and the position sensor and velocity sensor selection matrices $C_s^p \in \mathbb{R}^{n_y^p \times n}$ and $C_s^v \in \mathbb{R}^{n_y^v \times n}$. Please note that the velocities in δy are already global values as their local equilibrium values are always zero. In contrast, the global support position is given by the sum of its local value in δy and its local equilibrium value $y_0^C(\alpha)$.

At this point, from (9) and (10) it is evident, that the transformation angle α can be chosen as scalar scheduling parameter ρ. Thus, by inserting the measured global support position y_C into (1), the scheduling parameter can be calculated online and used to schedule the model matrices. Please note, that with this choice, the scheduling parameter depends on y_C and thus on the modal states. In order to avoid induced dynamics due to this state-dependency, y_C is low pass filtered for the calculation of the scheduling parameter with a cut off frequency below the first eigenfrequency. This way, the model is scheduled over the static displacements of the support without the influence of the modal vibrations (see also Jirasek et al. (2019b)).

3.4 Derivation of a Polytopic LPV Model

In a second step, the entries of the reduced order state-space matrices are approximated by polynomials of second order. This leads to matrices depending polynomially on the scheduling parameter, e.g. for the system matrix this results in

$$A(\alpha) = \mathcal{A}_0 + \alpha\mathcal{A}_1 + \alpha^2\mathcal{A}_2. \tag{11}$$

In order to establish a model with affine dependence, the scheduling parameter vector $\rho = [\rho_1 \ \rho_2]^T$ is introduced, with $\rho_1 = \alpha$ and $\rho_2 = \alpha^2 = \rho_1^2$. This yields state-space matrices with affine dependence on the scheduling parameters, e.g.

$$A(\rho) = \mathcal{A}_0 + \rho_1\mathcal{A}_1 + \rho_2\mathcal{A}_2. \tag{12}$$

However, note that this manipulation increases the number of scheduling parameters. The scheduling parameters $\rho_1 \in [\rho_{1,min} \dots \rho_{1,max}]$ and $\rho_2 \in [\rho_{2,min} \dots \rho_{2,max}]$ range in the rectangular polytope $\mathcal{P}$. This polytope can be tightened by incorporating the known quadratic relation between the two scheduling parameters (Ballesteros et al. (2013)). This leads to a reduced triangular polytope $\mathcal{P}_R$ with $M = 3$ vertices

$$\begin{aligned} \rho_{v1} &= [\rho_{1,min} \ \ \rho_{2,min}]^T, \\ \rho_{v2} &= \begin{bmatrix} \dfrac{\rho_{1,min}+\rho_{1,max}}{2} & \rho_{1,min}\cdot\rho_{1,max} \end{bmatrix}^T, \\ \rho_{v3} &= [\rho_{1,max} \ \ \rho_{2,max}]^T. \end{aligned} \tag{13}$$

The state-space matrices of (9) and (10) are then given in polytopic LPV form by

$$\begin{bmatrix} A(\rho) & [\, B_1(\rho) \ \ B_2(\rho)\,] \\ C(\rho) & 0 \end{bmatrix} = \sum_{i=1}^{3} \lambda_i \begin{bmatrix} A_{vi} & B_{vi} \\ C_{vi} & 0 \end{bmatrix} \tag{14}$$

with the vertex matrices

$$\begin{aligned} A_{vi} &= A(\rho_{vi}),\ B_{vi} = [\, B_1(\rho_{vi}) \ \ B_2(\rho_{vi})\,], \\ C_{vi} &= C(\rho_{vi}). \end{aligned} \tag{15}$$

For a given vector of scheduling parameters ρ_a, the convex coordinates λ_i can be calculated, such that (3) is fulfilled, which can be stated in matrix form as (see Ballesteros et al. (2013))

$$\begin{bmatrix} \lambda_1 \\ \lambda_2 \\ \lambda_3 \end{bmatrix} = \begin{bmatrix} \rho_{v1} & \rho_{v2} & \rho_{v3} \\ 1 & 1 & 1 \end{bmatrix}^{-1} \begin{bmatrix} \rho_{a,1} \\ \rho_{a,2} \\ 1 \end{bmatrix}. \tag{16}$$

4. CONTROL DESIGN

4.1 Control Structure

An overview of the structure for controller synthesis in terms of a generalized plant P with controller K is given in Fig. 4. The plant G was derived in the previous Section

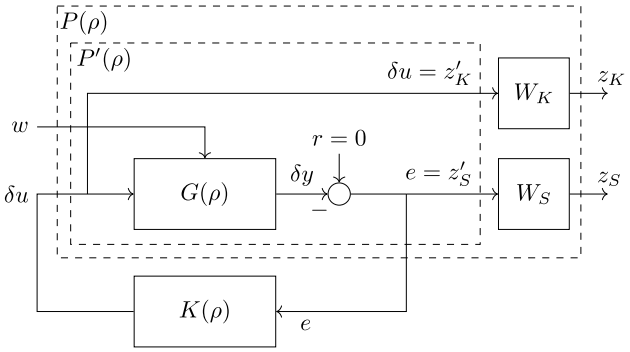

Fig. 4. Generalized plant for controller synthesis and controller.

with disturbance input w, local input δu and global output y. Notice that for control design the plant G is considered to only provide velocities as outputs and thus $y = \delta y$. Moreover, the transformation is assumed to be slow and hence the term $u_{ff} - u_0(\rho)$ of the input force is small and neglected. Then, the control signal generated by the controller is $u_k = \delta u$ (cp. Fig. 3). The performance outputs z_K and z_S of the generalized plant are weighted versions of the control signal δu and the control error $e = r - \delta y$, respectively, where we want the velocities to be zero and thus $r = 0$. Introducing the measurement matrix for velocities only $C_1(\rho) = [0 \quad C_s^v\Phi]$, the unweighted generalized plant P' can be written in state-space form as

$$\begin{bmatrix} \dot{x} \\ \hline z_S' \\ z_K' \\ \hline e \end{bmatrix} = \left[\begin{array}{ccc} A(\rho) & B_2(\rho) & B_1(\rho) \\ \hline -C_1(\rho) & 0 & 0 \\ 0 & 0 & 1 \\ \hline -C_1(\rho) & 0 & 0 \end{array}\right] \begin{bmatrix} x \\ w \\ \delta u \end{bmatrix}. \tag{17}$$

Then, the aim of controller synthesis is to find a controller K given by

$$\begin{bmatrix} \dot{x}_k \\ \delta u \end{bmatrix} = \begin{bmatrix} A_k(\rho) & B_k(\rho) \\ C_k(\rho) & D_k(\rho) \end{bmatrix} \begin{bmatrix} x_k \\ e \end{bmatrix}, \tag{18}$$

which minimizes the effect of the harmonic disturbance w on z_S and z_K in terms of the $\mathcal{H}_\infty$ norm (i.e. minimizing the RMS gain). With the transfer function from w to z

$$z(s) = \begin{bmatrix} z_S(s) \\ z_K(s) \end{bmatrix} = \begin{bmatrix} -W_S S G_w \\ -W_K K S G_w \end{bmatrix} w(s), \tag{19}$$

this can be expressed by

$$\gamma = \min_{K} \left\| \begin{bmatrix} W_S S G_w \\ W_K K S G_w \end{bmatrix} \right\|_\infty . \tag{20}$$

Here, $S = (I + G_u K)^{-1}$ is the sensitivity, and $G_u(s)$ and $G_w(s)$ are the transfer functions in the frozen sense from δu to δy and from w to δy, which are hidden inside G in Fig. 4. The weighting filters W_S and W_K are used to shape SG_w and KSG_w. If $\gamma < 1$, then the inverse weightings act as upper bounds on SG_w and KSG_w (Werner (2017)).

4.2 Polytopic LPV Controller

Following Apkarian et al. (1995) a polytopic LPV output-feedback controller can be found, guaranteeing stability and $\mathcal{H}_\infty$ performance γ between the disturbance input w and performance outputs z, if a positive definite matrix $X > 0$ and vertex controllers

$$\begin{bmatrix} A_k(\rho_{vi}) & B_k(\rho_{vi}) \\ C_k(\rho_{vi}) & D_k(\rho_{vi}) \end{bmatrix} \tag{21}$$

exist, such that for the vertices $i = 1, 2, \ldots, M$ the following holds

$$\begin{bmatrix} A_{cl}^T(\rho_{vi})X + X A_{cl}(\rho_{vi}) & X B_{cl}(\rho_{vi}) & C_{cl}^T(\rho_{vi}) \\ B_{cl}^T(\rho_{vi})X & -\gamma I & D_{cl}^T(\rho_{vi}) \\ C_{cl}(\rho_{vi}) & D_{cl}(\rho_{vi}) & -\gamma I \end{bmatrix} < 0, \tag{22}$$

where A_{cl}, B_{cl}, C_{cl} and D_{cl} are the matrices of the closed-loop between generalized plant P and controller K. Moreover, two assumptions on the generalized plant in (17) have to be satisfied, which are (i) the input matrix related to δu ($B_1(\rho)$) and the output matrix related to x ($C_1(\rho)$) are parameter independent, which is obviously not the case. In order to satisfy this assumption, a pre-filter is applied to the input δu and a post-filter is applied to the output δy of the plant G. This introduces additional filter states to the generalized plant in (17) and leads to an augmented generalized plant with a reconfiguration of the matrices, such that input and output matrix are parameter independent. For this augmented generalized plant, the second assumption (ii) requires quadratic stabilizability of the system matrix and the parameter independent input matrix and quadratic detectability of the system matrix and parameter independent output matrix. This assumption is fulfilled, as there are only stable filter and weighting matrices introduced to the augmented generalized plant and the original system has no unstable modes.

Returning to condition (22), notice that this is not a Linear Matrix Inequality (LMI) in the controller variables and X, because of the terms XA_{cl} and XB_{cl} (Werner (2018)). The manipulations needed to transfer (22) into an LMI are described in Apkarian et al. (1995), where an elimination approach is used to solve the problem. The controller can be synthesized using `hinfgs` of the Robust Control Toolbox from Matlab (see, e.g. Gu (2013) and Gahinet et al. (1995)). The resulting controller is then given in polytopic LPV form by

$$\begin{bmatrix} A_k(\rho) & B_k(\rho) \\ C_k(\rho) & D_k(\rho) \end{bmatrix} = \sum_{i=1}^{3} \lambda_i \begin{bmatrix} A_{k,vi} & B_{k,vi} \\ C_{k,vi} & D_{k,vi} \end{bmatrix}. \tag{23}$$

Once the vertex controllers are obtained, the controller matrices for an arbitrary scheduling parameter vector ρ_a can be calculated from the vertex controllers.

4.3 Filter, Weight Selection and Controller Synthesis

The pre- and post-filter are chosen as first order low-pass filters with bandwidth of 100 Hz, i.e. higher than the desired system bandwidth, so that their effect is negligible (see Apkarian et al. (1995)).

An essential part of the controller design is the choice of the weighting filters W_S and W_K. The filters are chosen such that the following aims are fulfilled (i) disturbances w that lie in the frequency range of the eigenfrequencies (0.5-10 Hz) are rejected and (ii) the controller does not react to low frequency disturbances due to the transformation of the structure. To achieve these requirements, the following weighting filters are chosen

$$\begin{aligned} W_S &= \frac{1.885 \cdot 10^4}{s + 188.5} \cdot \begin{bmatrix} 1 & 0 \\ 0 & 1 \end{bmatrix}, \\ W_K &= \frac{1 \cdot 10^5 s^2 + 7.854 \cdot 10^6 s + 1.421 \cdot 10^8}{41.67 s^2 + 2.094 \cdot 10^8 s + 1.184 \cdot 10^7}. \end{aligned} \tag{24}$$

With this choice of weighting filters, the controller can be synthesized and the result for the bound on the $\mathcal{H}_\infty$ norm is given by $\gamma = 0.9687$. The resulting sensitivity and control sensitivity together with the inverse weighting filters are depicted in Fig. 5. It can be seen that the inverse weights are indeed upper bounds on sensitivity and control sensitivity.

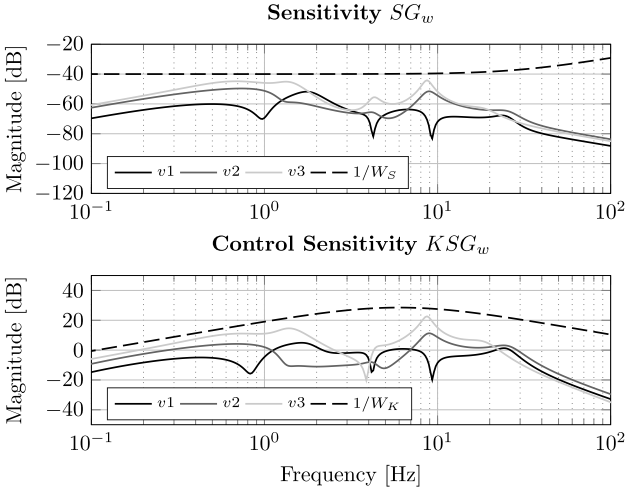

Fig. 5. Sensitivity (SG_w) and control sensitivity (KSG_w) for the 3 vertices vi and inverse weighting filters.

5. SIMULATION RESULTS

Simulations are conducted following the structure in Fig. 3. Simulation results for a transformation trajectory α_{ref} made up of ramp signals ($8° \nearrow 28° \nearrow 37° \searrow 17° \searrow 8°$) under a constant harmonic disturbance force w are depicted in Fig. 6. The trajectory is generated by an appropriate feed-forward force u_{ff}. The harmonic disturbance w is chosen such that the first (second, third, fourth) mode is excited with an amplitude of 20 N (200 N, 50 N, 10 N) and a constant frequency equal to $f_{20°,1} = 0.52$ Hz ($f_{20°,2} = 1.66$ Hz, $f_{20°,3} = 4.81$ Hz, $f_{20°,4} = 9.16$ Hz). The harmonic disturbance is active from 10 to 63 seconds. The results show that the vibrations can be reduced in all four modes and thus in the tip point velocities as well.

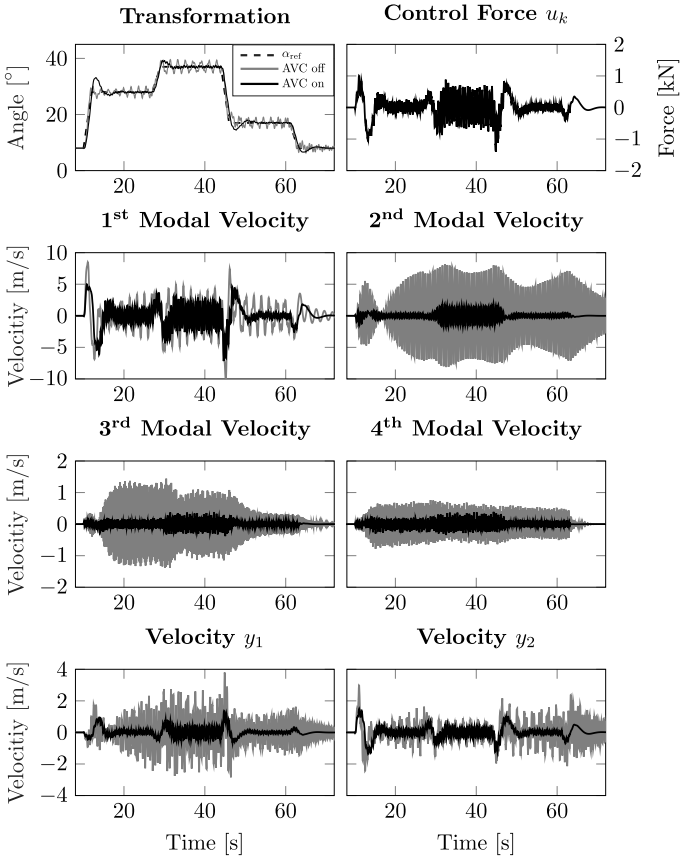

Fig. 6. Simulation results by means of modal velocities and tip point velocities with AVC off (—) and AVC on (**—**).

6. CONCLUSIONS AND FUTURE WORKS

A polytopic LPV model of a lightweight convertible structure was established, based on local linear models for discrete transformation states. This model was then used to synthesize a polytopic LPV output-feedback controller. Note that the designed controller guarantees stability and performance of the closed-loop only in the neighborhood of the local linear models and for slow changes of the operating point. For the simulated trajectory, the controller performed satisfying, but did not significantly improve the results of the previous SISO controller design (see Jirasek et al. (2019a)). However, the approach allows for much more flexibility by the selection of weighting functions and offers a huge potential for improvements in future implementations, such as the choice of more complex weighting functions and of weighting functions depending on the scheduling parameters. In addition, the results might be improved by lowering the level of conservatism through a tighter parameter polytope and the use of a parameter-dependent Lyapunov function for controller synthesis.

REFERENCES

Apkarian, P., Gahinet, P., and Becker, G. (1995). Self-scheduled $\mathcal{H}_\infty$ control of linear parameter-varying systems: a design example. *Automatica*, 31(9), 1251–1261.

Ballesteros, P., Shu, X., Heins, W., and Bohn, C. (2013). Reduced-order two-parameter pLPV controller for the rejection of nonstationary harmonically related multisine disturbances. In *Control Conference (ECC), 2013 European*, 1835–1842. IEEE.

Bleicher, A., Schlaich, M., and Schauer, T. (2011). Multimodal and multivariable active vibration control for a footbridge – model-based design and experimental validation. In *8th International Conference on Structural Dynamics (EURODYN)*, 1525–1532. Leuven.

Briat, C. (2015). *Linear Parameter-Varying and Time-Delay Systems*, volume 3 of *Advances in Delays and Dynamics*. Springer Berlin Heidelberg, Berlin, Heidelberg.

Gahinet, P., Nemirovski, A., Laub, A.J., and Chilali, M. (1995). *LMI Control Toolbox*. The Mathworks.

Gu, D.W. (2013). *Robust control design with Matlab*. Advanced textbooks in control and signal processing. Springer, New York, 2nd edition.

Hoffmann, C. and Werner, H. (2015). A Survey of Linear Parameter-Varying Control Applications Validated by Experiments or High-Fidelity Simulations. *IEEE Transactions on Control Systems Technology*, 23(2), 416–433.

Jirasek, R., Schauer, T., and Bleicher, A. (2019a). Active Vibration Control of a Convertible Structure based on a Linear Parameter-Varying Model. *IFAC-PapersOnLine*, 52(28), 190–195. doi:10.1016/j.ifacol.2019.12.375.

Jirasek, R., Schauer, T., and Bleicher, A. (2019b). Linear Parameter-Varying Models for Convertible Structures in Civil and Structural Engineering. *IFAC-PapersOnLine*, 52(15), 555–560. doi:10.1016/j.ifacol.2019.11.734.

Körner, A., Born, L., Mader, A., Sachse, R., Saffarian, S., Westermeier, A.S., Poppinga, S., Bischoff, M., Gresser, G.T., Milwich, M., Speck, T., and Knippers, J. (2018). Flectofold—a biomimetic compliant shading device for complex free form facades. *Smart Materials and Structures*, 27(1).

Lienhard, J., Alpermann, H., Gengnagel, C., and Knippers, J. (2013). Active Bending, a Review on Structures where Bending is Used as a Self-Formation Process. *International Journal of Space Structures*, 28(3-4), 187–196.

Mohammadpour, J. and Scherer, C.W. (eds.) (2012). *Control of Linear Parameter Varying Systems with Applications*. Springer US, Boston, MA.

Neuhäuser, S., Haase, W., Weickgenannt, M., and Sawodny, O. (2013). Adaptive Tragwerke – Aktuelle Forschungen im Ultraleichtbau. *Stahlbau*, 82(6), 428–437.

Senatore, G., Duffour, P., Winslow, P., and Wise, C. (2018). Shape control and whole-life energy assessment of an 'infinitely stiff' prototype adaptive structure. *Smart Materials and Structures*, 27(1).

Takahashi, K., Körner, A., Koslowski, V., and Knippers, J. (2016). Scale effect in bending-active plates and a novel concept for elastic kinetic roof systems. *Proceedings of IASS Annual Symposia*, 2016(16), 1–10.

Vergauwen, A., Laet, L.D., and Temmerman, N.D. (2017). Computational modelling methods for pliable structures based on curved-line folding. *Computer-Aided Design*, 83, 51–63.

Werner, H. (2017). *Optimal and Robust Control*. Lecture Notes, Hamburg University of Technology.

Werner, H. (2018). *Advanced Topics in Control*. Lecture Notes, Hamburg University of Technology.